Electric-Field-Induced Paths in Multiferroic $BiFeO_3$ from Atomistic Simulations

S. Lisenkov*
Department of Physics, University of South Florida, Tampa, Florida 33620, USA

D. Rahmedov and L. Bellaiche
Department of Physics, University of Arkansas, Fayetteville, Arkansas 72701, USA
(Received 16 January 2009; published 23 July 2009)

Properties of $BiFeO_3$ under an electric field are simulated using an *ab initio*-based approach. Complex paths and anomalous phenomena occur, depending on the direction of the field. Examples of such phenomena are the rotations of the polarization and of the axis about which the oxygen octahedra tilt; isostructural transitions; disappearance and reappearance of the tilting of the oxygen octahedra; and reentrance into specific crystallographic classes.The magnetic order parameter is not always perpendicular to the polarization, especially when the tilting of the oxygen octahedra disappears. The governing ''rule'' is that the magnetic order parameter remains orthogonal to the axis about which the oxygen octahedra tilt.

DOI: 10.1103/PhysRevLett.103.047204 PACS numbers: 75.80.+q, 75.30.Kz, 75.40.Mg, 77.80.Fm

Multiferroics can exhibit coupled magnetic order and ferroelectricity [1,2], and are of huge interest [3–13] because of the possibility of controlling their magnetic properties by the application of an electric field. Pioneering works [5–7] have investigated such magnetoelectric effect in $BiFeO_3$ (BFO). Such remarkable experimental studies demonstrate that the direction of the magnetic order parameter can be switched from one $\langle 011 \rangle$ to *another* $\langle 011 \rangle$ direction by applying an electric field along $[00\bar{1}]$, through a change in the direction of the polarization. Such switching is believed to occur because the magnetic order parameter desires to remain perpendicular to the polarization.

Despite these advances, many features related to the effects of electric field on properties of BFO remain poorly understood or even unknown. For instance, one may wonder what are the precise crystallographic phases before and after the change in the polarization's direction occurs. Another unanswered question is how this switching affects the tilting of the oxygen octahedra—which is often overlooked in BFO despite its large role [10–12]. It is also of high importance to determine the *complete* structural path of BFO under electric fields lying along $[00\bar{1}]$. In particular, can new phases possessing new directions of the polarization and of the magnetic order parameter (e.g., not only along $\langle 011 \rangle$ directions for that latter) occur if one applies fields of higher magnitude than those used in Refs [5–7]? Similarly, the effect of applying an electric field along *other* crystallographic directions on properties of BFO is currently undocumented. Does such application still result in a precise control of the magnetic sublattice because of the orthogonality between the field-induced direction of the polarization and the direction of the magnetic order parameter? Can it also lead to new phenomena?

In this Letter, we address the problems mentioned above by using an *ab initio*-based approach. We reveal that the interplay between polarization, tilting of the oxygen octahedra, magnetic ordering and direction of the applied electric field results in complex paths and striking features, such as (i) the joint rotations of the polarization and of the axis about which the oxygen octahadra tilt; (ii) the existence of many different crystallographic states; (iii) isostructural phase transitions between monoclinic phases; (iv) disappearance and then reappearance of the oxygen octahedra tilting; and (v) re-entrance into some symmetry classes. We also discovered that the common belief that magnetic order parameter and polarization are always rigidly coupled (such as to form an angle of 90°) has to be revisited. In fact, we found that the governing ''rule'' is that the magnetic order parameter rotates to remain perpendicular to the electric-field-induced direction of the axis about which the oxygen octahedra tilt.

We use the recently developed effective Hamiltonian scheme of Ref. [13]. This scheme yields *finite-temperature* properties of relatively *large* systems, by using its total energy, E_{tot}, into Monte Carlo (MC) simulations. Such technique accurately reproduces the Curie and Neel temperatures, as well as, the intrinsic magnetoelectric coefficients of BFO [13]. It also predicts a rhombohedral $R3c$ *ground state* that exhibits (i) a polarization $\mathbf{P}$ pointing along the [111] direction, (ii) a tilting of the oxygen octahedra about the [111] axis; and (iii) a (G-type) antiferromagnetism characterized by a vector, $\mathbf{L}$, being *perpendicular* to the [111] direction [14]. Those predictions are consistent with both direct first-principles calculations [4,5] and experiments [5,10,12]. Note that BFO *bulk* is in fact *nearly* G-type antiferromagnetic (AFM), since it rather exhibits a cycloidal arrangement of the magnetic moments with a length around 640 Å [6,15]. Such cycloid does not exist in BFO *films* [8], and is not found in our simulations for bulks (because it likely requires much larger supercells than those used here or additional interactions to be incorporated into E_{tot}). Our results should thus be valid for relaxed BFO films. They also should qualitatively apply to BFO bulks, by making a one-to-one correspondence be-

tween the field-induced directions of the AFM vector to be predicted here and the directions of propagation of the cycloid to be measured.

Our numerical results correspond to the use of a $12 \times 12 \times 12$ periodic supercell (8640 atoms) under a *dc* electric field, **E**. The effect of an external static electric field on physical properties is included by adding a $\mathbf{P} \cdot \mathbf{E}$ term in the effective Hamiltonian [16,17]. We perform 500 000 MC sweeps to get converged results for all considered **E**. Relevant outputs of the MC procedure are the local mode ferroelectric (FE) vector **u** (which is directly proportional to the electrical polarization); the G-type AFM vector, **L**; and a vector, ω, characterizing the tilting of the oxygen octahedra, that is characterizing the antiferrodistortive (AFD) motions associated with the *R* point of the cubic first Brillouin zone [12,18]. Here, we apply an electric field, with a magnitude up to 100 MV/cm, along different directions at 10 K. All the chosen directions are *not* perpendicular to our initial **L**, which is along $[01\bar{1}]$ [14]. Such choice was made so that the AFM vector would have to *rotate* if it still desires to be perpendicular to the polarization at high electric field (because P should be along the field's direction at high enough field [16,17], as a result of the $\mathbf{P} \cdot \mathbf{E}$ term).

For instance, Figs. 1(a)–1(c) display the Cartesian components of **u**, ω, and **L**, respectively, as a function of the magnitude of the electric field, when the latter is applied along the $[00\bar{1}]$ direction—as in recent experiments [5–7]. The *x*, *y*, and *z* axes are chosen along the pseudocubic [100], [010], and [001] directions, respectively. Figure 1(a) shows that applying such field with a magnitude ranging between 0 and 14.2 MV/cm causes the *z* component of the polarization to decrease with the field's magnitude, *E*, while the other two Cartesian components of **P** are nearly unaffected. In other words, the polarization is along $[uuv]$ directions (with *u* larger than *v*) when *E* increases. Similarly, Fig. 1(b) indicates that the axis about which the oxygen octahedra are rotating follows the same directional trend, because of the coupling between FE and AFD degrees of freedom. Such behaviors imply that the corresponding field-induced space group is monoclinic *Cc*. Interestingly, Fig. 1(c) reveals that the antiferromagnetic vector *rotates* from $[01\bar{1}]$ to $[\bar{1}10]$ when increasing *E* within this *Cc* phase, in order to maintain its orthogonality with the polarization and with the axis about which the oxygen octahedra tilt (see the inset of Fig. 1(c) showing the angle between **L** and **P**, and the angle between **L** and ω). Moreover, at the critical field $E_{c1} = 14.2$ MV/cm [19], a *first-order* transition occurs, resulting in the sudden change in sign of the *z* component (i) of the polarization, while the other two components of **P** remain unchanged—as precisely observed in Ref. [7]; and (ii) of the AFD vector, ω, to allow the oxygen octahedra to continue to rotate about an axis close (but not equal) to the polarization's direction. Note that, unlike commonly believed [5–7], **P** is *not* parallel to the $[11\bar{1}]$ direction just after E_{c1}, but rather lies along a $[uu\bar{v}]$ direction with *u* now being smaller than *v*.

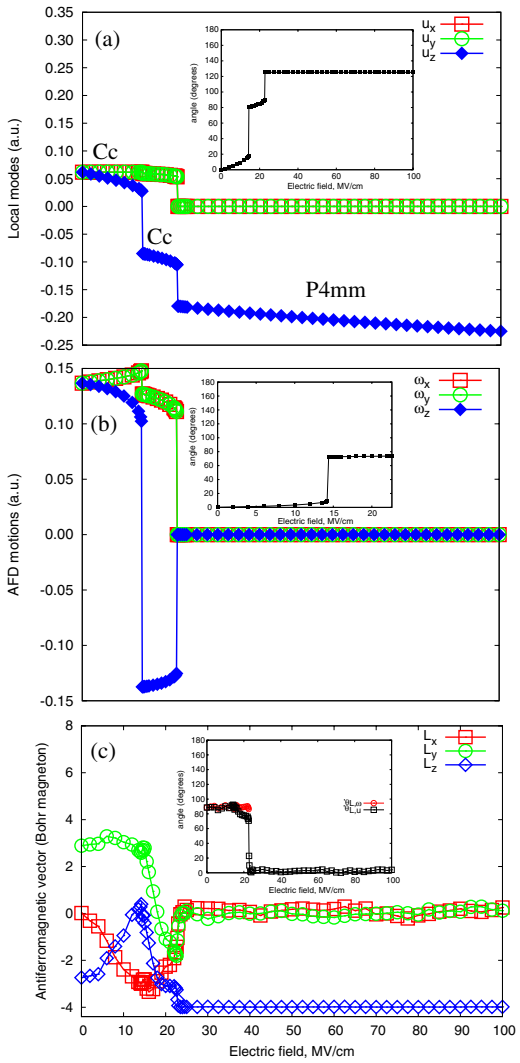

FIG. 1 (color online). Local modes [panel (a)], AFD-related quantity [panel (b)] and antiferromagnetic moment [panel (c)] of $BiFeO_3$ at 10 K as a function of the magnitude of an electric field applied along the $[00\bar{1}]$ direction. Insets of panels (a) and (b) show the angle between the polarization and the [111] direction, and the angle between ω and the [111] direction, respectively. The inset of panel (c) displays the angle between **L** and **P** (via open squares) and the angle between **L** and ω (via open circles).

The resulting space group is therefore still monoclinic *Cc*, implying that the phase transition occurring at E_{c1} is *isostructural*—which is rather rare in nature (see Ref. [20] and references therein). Moreover, at this critical field E_{c1}, **L** is still perpendicular to **P** and is different from its initial direction—as consistent with the measurements of Refs. [5–7] for the direction of the AFM vector in BFO films and for the direction of the propagation of the cycloid in BFO bulks.

Having successfully compared our predictions with measurements for low fields, we now focus on fields that are higher than E_{c1}. Figure 1 further reveals that another first-order transition occurs at a second critical field $E_{c2} = 22.8$ MV/cm. Above that field, the AFD distortions com-

pletely disappear while **P** is now parallel to **E**. This generates a P4mm tetragonal phase. Interestingly, Fig. 1(c) and its insets indicate that **L** is *not* orthogonal anymore to **P** for fields above E_{c1}, which is against a common belief [5–7]. In fact, one can clearly see that, between E_{c1} and E_{c2}, the behavior of **L** is governed by its desire to remain orthogonal to the axis about which the oxygen octahedra tilt, and that **L** is *parallel* to **P** above E_{c2}. Such unexpected findings are in fact consistent with Ref. [11], which suggests that a rigid and ''perpendicular'' coupling between magnetic ordering and AFD degrees of freedom is responsible for a weak ferromagnetism in BFO systems. Figure 1 thus predicts that three different field regions, each corresponding to different qualitative behaviors for the FE, AFD and magnetic degrees of freedom exist in BFO when applying a field along the $[00\bar{1}]$ direction.

Let us now investigate fields applied along $\langle 111\rangle$ pseudocubic directions that are *not* perpendicular to the initial ($[01\bar{1}]$) direction of **L**. Interestingly, these $\langle 111\rangle$ directions can be classified as belonging to two different classes, depending on the angle they form with the initial ([111]) direction of ω. *Class 1* gathers the $[1\bar{1}1]$ and $[11\bar{1}]$ directions that both exhibit an angle of 71° with respect to [111]. On the other hand, *Class 2* is formed by $[\bar{1}\,\bar{1}\,1]$ and $[\bar{1}1\bar{1}]$, which are directions having an angle of 109° degrees with respect to [111]. Figures 2(a)–2(c) display **u**, ω and **L**, respectively, as a function of the magnitude of the electric field, when the latter is applied along the $[1\bar{1}1]$ direction (Class 1). Figures 2(d)–2(f) show similar data but when **E** lies along $[\bar{1}\,\bar{1}\,1]$ (Class 2). One can clearly see that applying a field belonging to Class 1 and with a magnitude ranging between 0 and 18.4 MV/cm induces a rotation of both **P** and ω from [111] towards a $\langle 101\rangle$ direction, via $\langle uvu\rangle$ directions—with u larger than v. The resulting phase is of monoclinic Cc symmetry. Within this phase, the AFM vector also rotates when E increases, in order to remain orthogonal to ω (and also to the polarization). The situation dramatically differs for electric field above 18.4 MV/cm, which is the critical value at which a first-order transition occurs between the Cc phase and a rhombohedral $R3c$ state. In this latter structure, **P** now points along the field and increases in magnitude when E increases, while the tilting of the oxygen octahedra also occurs about the applied field's direction but decreases in magnitude with E—since an electric field favors polarization and that AFD and FE degrees of freedom fight each other [21]. Within this field-induced $R3c$ phase, the AFM vector is now along the $[10\bar{1}]$ direction, in order to continue to be orthogonal to the induced ω (but also to the induced polarization).

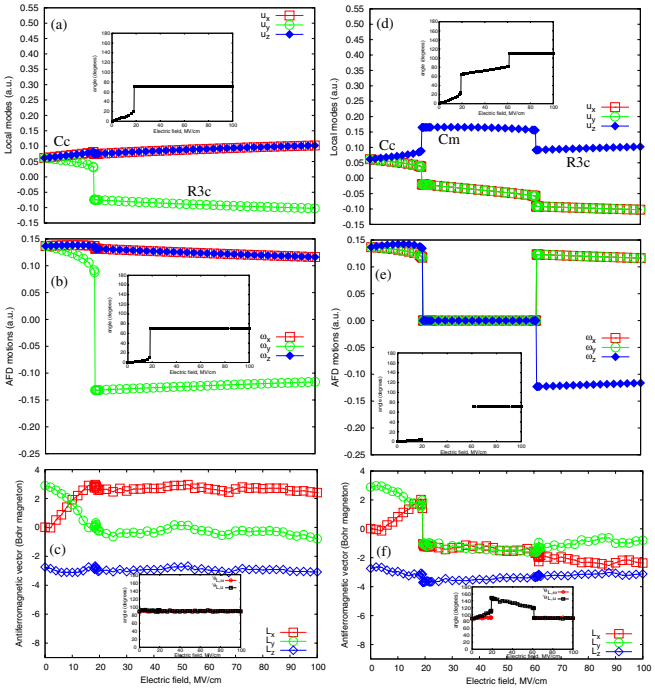

FIG. 2 (color online). Panels (a)–(c) and (d)–(f): Same as Fig. 1 but for a field applied along the $[1\bar{1}1]$ and $[\bar{1}\,\bar{1}\,1]$ direction, respectively.

Comparing Figs. 2(a)–2(c) with Figs. 2(d)–2(f) further reveals that the most striking novel feature related to Class 2 (with respect to Class 1) is the appearance of a new, intermediate phase in between the Cc state occurring at the lowest fields and the $R3c$ state happening for larger fields. This intermediate phase is characterized by the *complete annihilation* of the AFD vector while **P** is along a $\langle uuv\rangle$ direction, with u smaller than v in magnitude. Such intermediate phase is of monoclinic Cm symmetry. The annihilation of ω in the Cm state is numerically found to originate from the fact that FE and AFD degrees of freedom do not want to coexist when one component of the polarization is much larger in magnitude than the other two (note also that the magnitude of **P** is significantly increased at the Cc-to-Cm transition because of the complete suppression of the AFD motions). Increasing the magnitude of the electric field lying along $[\bar{1}\,\bar{1}\,1]$ up to a second critical value of 61.2 MV/cm leads to the transition from this Cm state to a $R3c$ phase for which the three components of **P** are equal to each other in magnitude, which therefore allows the *reappearance* of the AFD vector. During this whole complex path, Fig. 2(f) and its inset reveal that the AFM vector once again adapts itself to remain perpendicular to ω (when the tilting of the oxygen octahedra exists), rather than to **P** (see, for instance, that the angle between **L** and **P** ranges between 120° and 160° in the Cm phase). Figures 1 and 2 thus predict that BFO under electric fields can follow a rather rich structural path as a result of the interplay between **P**, ω, **L**, and **E**.

This is even more pronounced, when looking at Figs. 3(a)–3(c), that correspond to a field applied along the $[\bar{1}\,\bar{1}\,0]$ direction. As a matter of fact, four different regions exist in that case, for E up to 100 MV/cm. They are: (1) a monoclinic Cc region for which both **P** and ω are along (slightly different) $[uuv]$ directions with u smaller than v when E is less than 16.2 MV/cm; (2) another monoclinic Cc region when $16.2 < E < 42.6$ MV/cm,

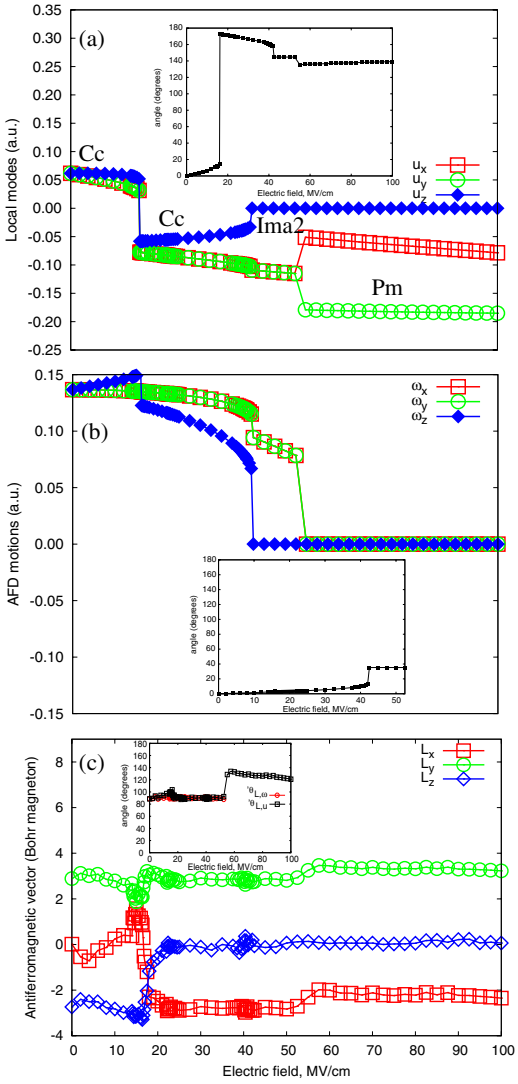

FIG. 3 (color online). Same as Fig. 1 but for a field applied along the $[\bar{1}\,\bar{1}\,0]$ direction.

with *all* the Cartesian components of **P** having reversed their sign with respect to the initial polarization; (3) an orthorhombic Ima2 phase in which a polarization lying along the field's direction coexists with the rotation of the oxygen octahedra about that field's direction for $42.6 < E < 55.0$ MV/cm; and (4) the *re-entrance* to the monoclinic symmetry, but with a *Pm* phase, for which the AFD distortions are completely annihilated while **P** lies along a $[\bar{u}\,\bar{v}\,0]$ direction [22], when $E > 55.0$ MV/cm. During this complex structural path, the AFM vector once again evolves, in order to remain perpendicular to ω (rather than to the polarization) for fields below 55.0 MV/cm. For higher fields, the tilting of the oxygen octahedra has vanished, leading to **L** lying along $[\bar{1}10]$ and thus forming an angle of 120° with **P**.

We are confident that our findings are of high fundamental and technological importance, and deepen our knowledge of the fascinating fields of multiferroics.

This work is supported by ONR Grants No. N00014-04-1-0413 and No. N00014-08-1-0915, NSF Grants No. DMR-0701558, No. DMR-0404335 and No. DMR-0080054. S. L. acknowledges the support from the University of South Florida under Grant No. R074021. We also acknowledge the computational support provided by the NSF MRI Grant No. 072265, and by the HPCMO of the US DOD.

*slisenk@cas.usf.edu

[1] G. A. Smolenskii and I. E. Chupis, Sov. Phys. Usp. **25**, 475 (1982).
[2] W. Eerenstein, N. D. Mathur, and J. F. Scott, Nature (London) **442**, 759 (2006).
[3] N. A. Spaldin and M. Fiebig, Science **309**, 391 (2005).
[4] J. B. Neaton *et al.*, Phys. Rev. B **71**, 014113 (2005).
[5] T. Zhao *et al.*, Nature Mater. **5**, 823 (2006).
[6] D. Lebeugle *et al.*, Phys. Rev. Lett. **100**, 227602 (2008).
[7] S. Lee *et al.*, Phys. Rev. B **78**, 100101(R) (2008).
[8] H. Bea *et al.*, Appl. Phys. Lett. **87**, 072508 (2005); H. Bea *et al.*, Philos. Mag. Lett. **87**, 165 (2007).
[9] R. Mazumder *et al.*, Appl. Phys. Lett. **91**, 062510 (2007).
[10] R. Haumont *et al.*, Phys. Rev. B **73**, 132101 (2006).
[11] C. Ederer and N. A. Spaldin, Phys. Rev. B **71**, 060401(R) (2005).
[12] I. A. Kornev *et al.*, Phys. Rev. Lett. **99**, 227602 (2007).
[13] S. Lisenkov, I. A. Kornev, and L. Bellaiche, Phys. Rev. B **79**, 012101 (2009).
[14] We numerically found that, for zero electric field, the magnetic anisotropy in the (111) plane is rather weak. As a result, the (zero-field) initial direction of the AFM vector, at low temperature, can sometimes differ from $[01\bar{1}]$, depending on the cooling procedure used.
[15] I. Sosnowska, T. P. Neumaier, and E. Steichele, J. Phys. C **15**, 4835 (1982).
[16] A. Garciá and D. Vanderbilt, Appl. Phys. Lett. **72**, 2981 (1998).
[17] L. Bellaiche, A. Garciá, and D. Vanderbilt, Phys. Rev. B **64**, 060103(R) (2001).
[18] I. A. Kornev *et al.*, Phys. Rev. Lett. **97**, 157601 (2006).
[19] The predicted E_{c1} is larger than the observed critical field of Refs. [5,7] (that are of the order of 0.02–0.2 MV/cm). Such discrepancy, which is likely related to the Landauer paradox [R. Landauer, J. Appl. Phys. **28**, 227 (1957).], may be due to the existence of inhomogeneities in the grown samples. Our simulated fields displayed in Figs. 1–3 should thus be decreased by 2 orders of magnitude, when comparing our predictions with measurements.
[20] V. Ranjan *et al.*, Phys. Rev. B **71**, 195302 (2005).
[21] D. Vanderbilt and W. Zhong, Ferroelectrics **206**, 181 (1998).
[22] This monoclinic Pm phase originates from the fact that BFO is numerically found to have a polarization lying along a $\langle 100\rangle$ direction rather than along a $\langle 110\rangle$ direction when the AFD degrees of freedom are frozen to zero, under no external field [I. A. Kornev and L. Bellaiche, Phys. Rev. B **79**, 100105(R) (2009)].